Brillouin distributed sensing using localized and stationary dynamic gratings

Nikolay Primerov[a], Yair Antman[b], Juan Sancho[a§], Avi Zadok[b], and Luc Thevenaz[*a]

[a]Ecole Polytechnique Fédérale de Lausanne, Institute of Electrical Engineering, SCI-STI-LT Station 11, 1015 Lausanne, Switzerland;
[b]Faculty of Engineering, Bar-Ilan University, Ramat-Gan 52900 Israel;
[§]Permanent address: iTEAM Institute, Universidad Politécnica de Valencia, 46022 Valencia, Spain.

ABSTRACT

In this work, we apply a recent technique for the generation of stimulated Brillouin scattering (SBS) dynamic gratings that are both localized and stationary to realize high-resolution distributed temperature sensing. The gratings generation method relies on the phase modulation of two pump waves by a common pseudo-random bit sequence (PRBS), with a symbol duration that is much shorter than the acoustic lifetime. This way the acoustic wave can efficiently build up in the medium at discrete locations only, where the phase difference between the two waves does not temporarily vary. The separation between neighboring correlation peaks can be made arbitrarily long. Using the proposed method, we experimentally demonstrate distributed temperature sensing with 5 cm resolution, based on modifications to both the local birefringence and the local Brillouin frequency shift in polarization maintaining fibers. The localization method does not require wideband detection and can generate the grating at any random position along the fiber, with complete flexibility. The phase-coding method is equally applicable to high-resolution SBS distributed sensing over standard fibers.

Keywords: Stimulated Brillouin scattering; distributed fiber sensors; nonlinear fiber optics; dynamic acoustic gratings; polarization maintaining fibers.

1. INTRODUCTION

Stimulated Brillouin scattering (SBS) is a nonlinear optical phenomenon that couples between two counter-propagating waves[1]. The combined intensity of the two waves added together drives an acoustic wave in the medium, whose frequency Ω matches the difference between the two optical frequencies[1]. The acoustic wave is accompanied by a traveling grating of refractive index variations, which could couple between the two optical waves. Effective buildup of the acoustic wave, and hence effective optical coupling, could only occur when Ω matches the Brillouin frequency shift Ω_B of the optical medium[1]. The value of Ω_B in standard single-mode fibers is on the order of $2\pi\cdot11$ GHz. The relatively long lifetime $\tau \sim 6$ ns of the acoustic wave decrees that Ω must fall within a few tens of MHz from Ω_B for efficient SBS to take place[1]. SBS is observed in standard fibers for optical power levels as low as a few mW.

SBS has found practical and commercial application in distributed sensing along standard fibers that are attached to a structure under test[2-5]. Sensing is based on monitoring the local value of Ω_B, which varies with both temperature and mechanical strain[2-5]. In Brillouin optical time domain analysis (B-OTDA), an intense pump wave is used to amplify counter-propagating, typically weaker probe waves[6]. The position-dependent Ω_B is recovered through mapping the power of the amplified probe, as a function of both time and frequency detuning Ω. The measurement range of B-OTDA can reach tens of km, however its spatial resolution is fundamentally restricted to the order of 1 m by the acoustic lifetime: The use of either pump or probe pulses much shorter than τ leads to SBS amplification that is both weaker and spectrally broadened[7].

Over the last decade, several techniques have been proposed and demonstrated for improving B-OTDA resolution towards cm scale[8-9]. In one scheme, known as Brillouin optical correlation-domain analysis (B-OCDA), the

[*] Luc.Thevenaz@epfl.ch Tel.: +41 (0) 21 69 34774; Fax: +041 (0) 21 69 34660.

Optical Sensing and Detection II, edited by Francis Berghmans, Anna Grazia Mignani, Piet De Moor,
Proc. of SPIE Vol. 8439, 843908 · © 2012 SPIE · CCC code: 0277-786X/12/$18 · doi: 10.1117/12.922976

instantaneous frequencies of constant-magnitude pump and probe waves, that are nominally detuned by Ω, are synchronously modulated by a common sine wave[10-11]. Due to the modulation, the frequency difference between the two counter-propagating waves remains stationary at particular fiber locations only, known as correlation peaks, whereas the frequency difference elsewhere is oscillating[10-11]. Consequently, effective SBS amplification is restricted to the correlation peaks, and probe power measurements may convey localized information. When simple sine-wave frequency modulation is used, tight trade-offs prevail between the B-OCDA range and resolution[10-11]: The unambiguous measurement range of B-OCDA is restricted to the separation between periodic correlation peaks, which is only a few hundreds of resolution points. B-OCDA was recently extended to dual-tone frequency modulation, resulting in a measurement range of 1.5 km with 27 cm resolution[12]. Other techniques for resolution enhancement include the pre-excitation of the acoustic wave[13-15], the use of dark[16] and π-phase[17-18] pump pulses, double pump pulses having different widths[19], differentiation of the measured probe power[20] and more. High-resolution B-OTDA measurements were demonstrated using all of the above techniques, with measurement ranges reaching a few km. Many of the above methods, however, add considerable complexity to the measurement scheme. In spite of much effort and progress, cm-scale, long-reach SBS sensing remains challenging.

Over the last three years, SBS-based *dynamic acoustic gratings* over polarization maintaining (PM) fibers have been drawing increasing attention[21-33]. Dynamic gratings are introduced by two counter-propagating pump waves, separated in frequency by Ω_B and co-polarized along one principal axis of the PM fiber. The gratings can be switched on and off and moved along the fiber, through the timing and modulation the pump waves. The dynamic gratings are interrogated by a third, probe signal, which is polarized along the orthogonal principal axis of the PM fiber. Due to the relatively large birefringence of such fibers, the frequency of the reading signal must be detuned from those of the pumps, typically by a few tens of GHz[21]. The reading signal is back-reflected by the dynamic grating into a fourth wave, which can be measured to monitor the entire process.

Dynamic gratings have been drawing increasing interest in sensing applications. The spectral offset between the pump and readout waves varies with the PM fiber birefringence, which in turn depends on both temperature and strain. Dynamic gratings therefore add another dimension to B-OTDA sensing[22-25, 27-29, 32]: a change in strain or temperature modifies the readout probe frequency of maximum reflection, as well as the value of Ω_B. In one particular example, the sensitivities of the readout frequency offset to temperature and strain variations were found to be ~ -55 MHz/°C and +0.9 MHz/με, respectively[24-25]. Since the two sensitivities are of opposite signs, measurements of both the Brillouin gain spectrum and the fiber birefringence using dynamic gratings can remove the ambiguity between strain and temperature variations[27]. When two continuous wave (CW) pumps are used, a uniform dynamic grating is introduced along the entire PM fiber. Localized sensing using such extended gratings may still be possible, when they are interrogated by short readout probe pulses and high-bandwidth detectors[22-25, 27-29, 32]. Nonetheless, localized dynamic gratings would support distributed sensing with CW readout probes. Localized dynamic gratings have been generated using pump pulses[27, 33]. However, much like B-OTDA measurements in standard fibers, the generation of short gratings is restricted by the acoustic lifetime τ. In addition, the gratings must be 'refreshed' by periodic pump pulses every τ, and the strength of reflection is temporally varying. B-OCDA was also introduced to obtain localized dynamic gratings[25]. However, the frequency modulation of the two pumps introduces additional complexity, as the readout probe signal must be synchronously modulated as well[25].

In this work, we apply a novel, recently proposed method for the generation of stationary and localized dynamic gratings[34-38] to 5 cm-scale distributed temperature sensing over polarization maintaining fibers. The method relies on the phase modulation of the two pump waves by a common pseudo-random bit sequence (PRBS), with a symbol duration *T* that is much shorter than τ. Much like B-OCDA, the method allows for an effective SBS interaction in discrete, cm-scale correlation peaks only. The separation between neighboring correlation peaks, however, is governed by the length of the PRBS, and it is uncorrelated with the length of the localized gratings. We have previously employed this method in the long variable delay of probe read-out pulses[35-36, 38], and in the generation of tunable microwave-photonic filters[36-37]. Here we report the application of the technique to high-resolution distributed sensing over polarization maintaining fiber, in larger detail. Lastly, the technique is equally applicable to high-resolution SBS distributed sensing over standard single-mode fibers.

2. PRINCIPLE OF OPERATION

The principle underlying the generation of stationary and localized dynamic gratings was described in detail elsewhere[35], and will be repeated here only briefly. Let us denote the complex envelopes of the two pump waves of an SBS dynamic grating as $A_{1,2}(t,z)$, respectively, where t stands for time and z represents position along a PM fiber of length L. Pump A_1 enters the fiber at $z = 0$ and propagates along the positive z direction, whereas pump A_2 propagates from $z = L$ in the negative z direction. The optical frequencies of the two pump waves, $\omega_{1,2}$, are separated by $\Omega \sim \Omega_B$. The complex envelopes of the two waves are phase-modulated by a common PRBS with symbol duration T:

$$A_1(t, z=0) = A_2(t, z=L) = A(t) = A_0 \left\{ \sum_n \mathrm{rect}\left[(t - nT)/T \right] \exp(j\varphi_n) \right\} \tag{1}$$

In Eq. (1), φ_n is a random phase variable which equals either 0 or π, $\mathrm{rect}(\xi)$ equals 1 for $|\xi| < 0.5$ and zero elsewhere, and A_0 denotes the constant magnitude of both pump waves. The modulation is synchronized so that the phases of the two pumps, at their respective entry points into the fiber, are equal for all t. Both pumps are polarized along the same principal axis of the PM fiber, denoted as $\hat{\mathbf{x}}$.

Consider next the magnitude of the acoustic density wave $Q(t,z)$ of frequency Ω that is generated by the two pumps. The driving force for the acoustic wave is proportional to the product $A_1(t,z)A_2^*(t,z)$ [1, 35]. Within a short section surrounding the center of the fiber at $z = L/2$, the two modulated pump waves are correlated, hence the driving force for the acoustic grating generation is stationary and of constant phase. Consequently, the acoustic grating in this region is allowed to build up to its steady state magnitude. The width of the correlation peak is on the order of $\Delta z = \frac{1}{2} v_g T$, corresponding to the spatial extent of a single PRBS symbol. In all other z locations, on the other hand, the driving force is randomly alternating is sign due to the random phase change between 0 and π, on every symbol duration $T << \tau$. Over the lifetime τ, the integrated driving force for the acoustic field generation averages to a zero expectation value and the buildup of the acoustic field outside the correlation peak is inhibited. The separation between adjacent peaks equals $\frac{1}{2} M v_g T$, where M is the PRBS length. The unambiguous measurement range can be made arbitrarily long with increasing M, while retaining the above resolution of Δz. The correlation peaks, with the exception of the zeroth-order one, can be scanned across a fiber under test through changing the code length factor M or the symbol duration T. Since there is no frequency modulation of the pumps the spatial period of the acoustic grating does not oscillate, and the subsequent readout of the acoustic grating by a $\hat{\mathbf{y}}$ polarized interrogating wave becomes considerably simpler than in B-OCDA over PM fibers[25].

3. EXPERIMENTAL SETUP AND RESULTS

Figure 1 illustrates the experimental setup that was used for the generation and characterization of dynamic acoustic gratings, driven by random phase modulation of both pump waves[35-38]. A single distributed feed-back (DFB) laser diode of frequency ω_1 was used to generate both pump waves. The output of the pumps DFB was modulated by an electro-optic phase modulator (EOM), which was driven by a PRBS generator. The output peak-to-peak voltage of the PRBS generator was adjusted to match V_π of the EOM, and its clock rate was set to $1/T = 2$ GHz by a microwave generator. The PRBS symbol duration corresponds to a spatial resolution of ~ 5 cm.

The modulated DFB light was split in two arms. Light in one path was amplified by an erbium-doped fiber amplifier (EDFA) to $|A_1|^2 \sim 200$ mW, polarized along the $\hat{\mathbf{x}}$ principal axis of a PM fiber, and launched into a section of specialty PM fiber under test (FUT) as pump 1. Light in the other arm was modulated by a second EOM, which was driven by a sine wave of frequency $\Omega \sim 2\pi \cdot 10$ GHz from a second microwave generator. The EOM in this arm was biased to suppress the optical carrier at ω_1. The upper modulation sideband of frequency $\omega_2 = \omega_1 + \Omega$ was selected by a narrow-

band fiber Bragg grating (FBG), amplified by a second EDFA to $|A_2|^2 \sim 200$ mW, and launched along the $\hat{\mathbf{x}}$ axis from the opposite end of the FUT as pump 2. The residual carrier wave and the other modulation sideband of pump 2 were rejected by the FBG.

Light from a second DFB laser was used to generate the readout signal wave. The optical frequency of the signal DFB was adjusted via temperature and current control to match the frequency of maximum reflectivity of the acoustic dynamic grating along the $\hat{\mathbf{y}}$ principal axis[21, 35]:

$$\omega_{sig} = \omega_2 + \Delta\omega = \omega_2 + \frac{\Delta n}{n_g}\omega_2 \qquad (2)$$

Here, $\Delta n_g << 1$ is the difference between the group indices of propagation along $\hat{\mathbf{x}}$ and $\hat{\mathbf{y}}$ axes, and n denotes the mean value of the two indices. The readout CW signal was modulated by a 50 kHz sine-wave, polarized along the $\hat{\mathbf{y}}$ principal axis of the PM FUT, and was launched to probe the acoustic dynamic grating. The reflected signal of frequency $\omega_{read} = \omega_1 + \Delta\omega$ was filtered by another FBG, amplified and measured using either a low-bandwidth detector. The detected photo-current was monitored by a lock-in amplifier tuned to 50 kHz, in order to improve the measurement signal to noise ratio (SNR).

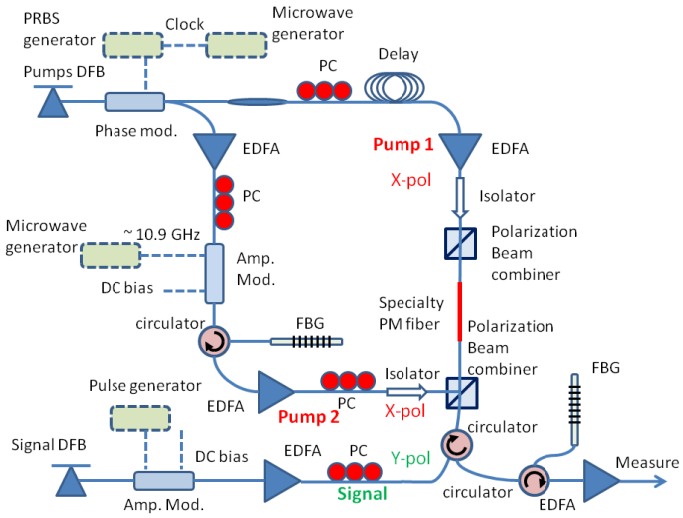

Fig. 1: Experimental setup for the generation and characterization of dynamic acoustic gratings, using SBS with phase-modulated pump waves. PC: polarization controller[35, 36].

A 5 cm-long section of the FUT was placed in contact with a high-current resistor, to generate a local hot-spot. The sensing measurements took advantage of the thermal variations in both the local birefringence in the PM FUT and its local Brillouin frequency shift. Figure 2 shows the relative power of the reflected readout signal, as a function of the dynamic grating position z and the detuning of the readout signal frequency ω_{sig} ('birefringence scan'). In one scan (left-hand panel), the frequency separation Ω between the two pumps was set to match Ω_B of the FUT at room temperature. The reflectivity peak is absent at the location of the hot spot. In a second scan (right-hand panel), Ω was readjusted to match the Brillouin frequency shift at the hot spot. The reflectivity peak is recovered, and obtained at a different readout frequency due to the change in the local birefringence.

Figure 3 shows the relative reflected power as a function of the grating position and the frequency separation Ω between the two SBS pumps ('Brillouin shift scan'). In the left-hand panel, the frequency of the readout probe wave ω_{sig} was adjusted to its value of maximum reflectivity at room temperature. Here too, the peak of the Brillouin gain spectrum is

absent at the hot spot. The peak is recovered at the scan depicted on the right-hand side, in which ω_{sig} was set to its value of peak reflectivity at the hot spot. The secondary peak at the first 20 cm of the FUT in the left-hand panel of Fig. 3 also appears in a background scan with no heating at all (not shown here). It is probably due to some damage strain in the FUT. The results of both birefringence and Brillouin scans successfully resolve the hot-spot, and recover its position to cm-scale accuracy. The sensing scheme does not require short readout pulses or broad bandwidth detection.

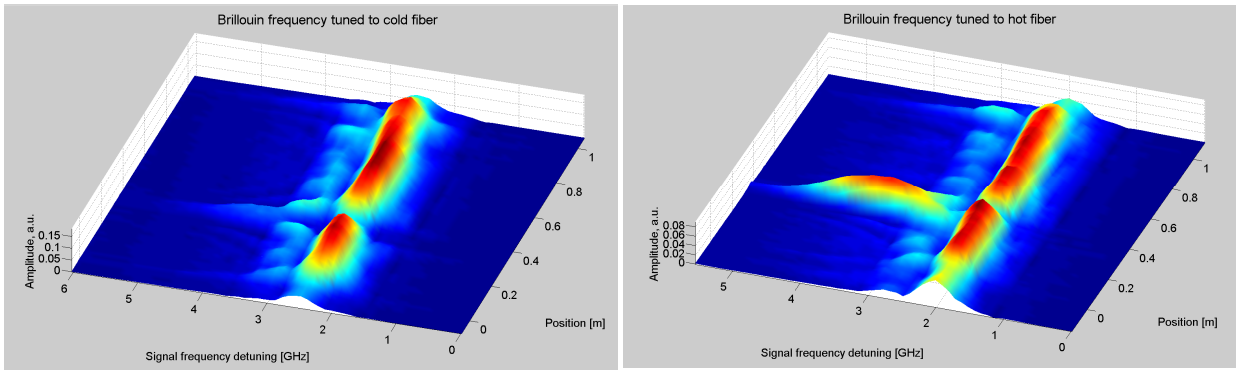

Fig. 2: Measurement of the relative power of a reflected readout signal from a 1 m long fiber under test, as a function of the position of the localized grating z and the shift of the readout signal frequency ω_{sig} from its value of maximum reflectivity at ambient conditions. A 5 cm-long hot-spot was generated along the fiber under test. Left – The frequency offset Ω between the two pumps was set to the Brillouin frequency shift of the fiber at room temperature. Right - Ω set to the Brillouin frequency shift at the hot spot.

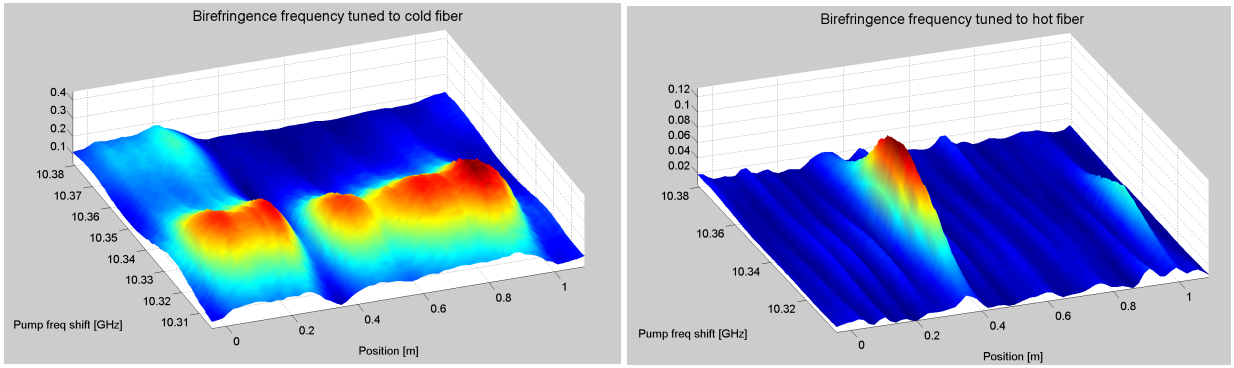

Fig. 3: Measurement of the relative power of a reflected readout signal from a 1 m long fiber under test, as a function of the position of the localized grating z and the frequency separation Ω between the pump waves. A 5 cm-long hot-spot was generated along the fiber under test. Left – The frequency of the readout probe wave ω_{sig} was set to its value of maximum reflectivity at room temperature. Right - ω_{sig} was set to its value of maximum reflectivity at the hot spot

4. CONCLUSIONS

High-resolution distributed temperature sensing over polarization maintaining fibers, using stationary and localized dynamic gratings, is experimentally demonstrated. The measurement range and resolution in the particular experiment were 1 m and 5 cm, respectively. Later experiments carried over standard fibers, which lie beyond the scope of this paper, had improved resolution to 1.2 cm and extended the measurement range to 40 m. There measurement range is scalable towards km, and it is decorrelated from the measurement resolution.

Measurements carried out using dynamic gratings over PM fibers provide the added value of monitoring both the local Brillouin frequency shift and the local birefringence. Unlike previous demonstration of dynamic grating-based sensing, the localized and stationary gratings were interrogated using low frequency modulated probe signals and low-bandwidth detectors. The underlying method was also employed in all-optical variable delay lines with a large delay-times-bandwidth product, and in tunable radio-frequency-photonic filters.

ACKNOWLEDGMENTS

This work was supported by the Swiss National Science Foundation through project 200021-134546, by the European Community's Seventh Framework Programme [FP7/2007–2013] under grant agreement no. 219299 (GOSPEL project), the Israeli Science Foundation (ISF), and by the KAMIN program of the Israeli Ministry of Industry, Trade and Labor. The work was realized in the collaborative framework of COST Action TD1001 OFSESA.

REFERENCES

[1] Boyd, R. W., [Nonlinear Optics], third edition, Academic Press (2008).
[2] Kurashima, T., Horiguchi, T., and Tateda, M., "Distributed-temperature sensing using stimulated Brillouin scattering in optical silica fibers," Opt. Lett. 15, 1038-1040 (1990).
[3] Horiguchi, T., Kurashima, T., and Tateda, M., "A technique to measure distributed strain in optical fibers," IEEE Photon. Technol. Lett. 2, 352-354 (1990).
[4] Bao, X., Webb, D. J., and Jackson, D. A., "22-km distributed temperature sensor using Brillouin gain in an optical fiber," Opt. Lett. 18, 552-554 (1993).
[5] Niklès, M., Thévenaz, L., and Robert, P. A., "Simple distributed fiber sensor based on Brillouin gain spectrum analysis," Opt. Lett. 21, 758-760 (1996).
[6] Horiguchi, T., and Tateda, M., "Optical fiber attenuation investigation using stimulated Brillouin scattering between a pulse and a continuous wave," Opt. Lett., 14, 408-410 (1989).
[7] Fellay, A., Thevenaz, L., Facchini, M., Nikles, M., and Robert, P., "Distributing sensing using stimulated Brillouin scattering: Toward ultimate resolution," in Proceedings of the Optical Fiber Sensors Conference (OFS-12), 324–327 (1997).
[8] Beugnot, J.-C., Tur, M., Foaleng Mafang, S., and Thévenaz, L., "Distributed Brillouin sensing with sub-meter spatial resolution: modeling and processing," Opt. Express 19, 7381-7397 (2011).
[9] Bao, X. and Chen, L. A., "Recent progress in Brillouin scattering based fiber sensors," Sensors 11, 4152-4187 (2011).
[10] Hotate, K., and Hasegawa, T., "Measurement of Brillouin gain spectrum distribution along an optical fiber using a correlation-based technique – proposal, experiment and simulation," IEICE Trans. Electron. E83-C, 405-412 (2000).
[11] Hotate, K., and Tanaka, M., "Distributed fiber Brillouin strain Sensing with 1-cm spatial resolution by correlation-based continuous-wave technique," IEEE Photon. Technol. Lett. 14, 179-181 (2002).
[12] Mizuno, Y., He, Z. Y., and Hotate, K., "Measurement range enlargement in Brillouin optical correlation-domain reflectometry based on double-modulation scheme," Optics Express 18, 5926-5933 (2010).
[13] Bao, X., Brown, A., Demerchant, M., and Smith, J., "Characterization of the Brillouin-loss spectrum of single-mode fibers by use of very short (<10-ns) pulses," Opt. Lett. 24, 510–512 (1999).
[14] Lecoeuche, V., Webb, D. J., Pannell, C. N., and Jackson, D. A., "Transient response in high-resolution Brillouin based distributed sensing using probe pulses shorter than the acoustic relaxation time," Opt. Lett. 25, 156–158 (2000).
[15] Wang, F., Bao, X., Chen, L., Li, Y., Snoddy, J., and Zhang, X., "Using pulse with dark base to achieve high spatial and frequency resolution for the distributed Brillouin sensor," Opt. Lett. 33, 2707-2709 (2008).
[16] Brown, A. W., Colpitts, B. G., and Brown, K., "Distributed Sensor Based on Dark-Pulse Brillouin Scattering," IEEE Photon. Technol. Lett. 17, 1501–1503 (2005).
[17] Thévenaz, L., and Foaleng Mafang, S., "Distributed fiber sensing using echoes", Proceedings of 19th International Conference of Fiber Sensors, (SPIE, Perth, WA, Australia)," Proc. SPIE 7004, 70043N, 70043N-4 (2008).

[18] Foaleng Mafang, S., Tur, M., Beugnot, J. C., and Thevenaz, L., "High spatial and spectral resolution long-range sensing using Brillouin echoes," Journal of Lightwave Technol. 28, 2993-3003 (2010).
[19] Li, W., Bao, X., Li, Y., and Chen, L., "Differential pulse-width pair BOTDA for high spatial resolution sensing," Opt. Express 16, 21616-21625 (2008).
[20] Sperber, T., Eyal, A., Tur, M., and Thevenaz, L., "High spatial resolution distributed sensing in optical fibers by Brillouin gain-profile tracing," Opt. Express 18, 8671–8679 (2010).
[21] Song, K. Y., Zou, W., He, Z., and Hotate, K., "All-optical dynamic grating generation based on Brillouin scattering in polarization-maintaining fiber," Opt. Lett. 33, 926-928 (2008).
[22] Dong, Y., Bao, X., and Chen, L., "Distributed temperature sensing based on birefringence effect on transient Brillouin grating in a polarization-maintaining photonic crystal fiber," Opt. Lett. 34, 2590-2592 (2009).
[23] Dong, Y., Chen, L., and Bao, X., "Truly distributed birefringence measurement of polarization- maintaining fibers based on transient Brillouin grating," Opt. Lett. 35,193-195 (2010).
[24] Zou, W., He, Z., and Hotate, K., "Complete discrimination of strain and temperature using Brillouin frequency shift and birefringence in a polarization-maintaining fiber," Opt. Express 17, 1248-1255 (2009).
[25] Zou, W., He, Z., Song, K. Y., and Hotate, K., "Correlation-based distributed measurement of a dynamic grating spectrum generated in stimulated Brillouin scattering in a polarization-maintaining optical fiber," Opt. Lett. 34, 1126-1128 (2009).
[26] Song, K. Y., Lee, K., and Lee, S. B., "Tunable optical time delays based on Brillouin dynamic grating in optical fibers," Opt. Express 17, 10344-10349 (2009).
[27] Dong, Y., Chen, L., and Bao, X., "High-spatial-resolution simultaneous strain and temperature sensor using Brillouin scattering and birefringence in a polarization-maintaining fibre," IEEE Photonic. Technol. Lett. 22, 1364-1366 (2010).
[28] Song, K. Y., Chin, S., Primerov N., and Thevenaz, L., "Time-domain distributed fiber sensor with 1 cm spatial resolution based on Brillouin dynamic grating," J. Lightwave Technol. 28, 2062-2067 (2010).
[29] Song K. Y., and Yoon, H. J., "High-resolution Brillouin optical time domain analysis based on Brillouin dynamic grating," Opt. Lett. 35, 52-54 (2010).
[30] Song K. Y., and Yoon, H. J., "Observation of narrowband intrinsic spectra of Brillouin dynamic gratings," Opt. Lett. 17, 2958-2960 (2010).
[31] Dong, Y., Chen, L., and Bao, X., "Characterization of the Brillouin grating spectra in a polarization-maintaining fiber," Opt. Express 18, 18960-18967 (2010).
[32] Chin, S., Primerov, N., and Thevenaz, L., "Sub-Centimeter Spatial Resolution in Distributed Fiber Sensing Based on Dynamic Brillouin Grating in Optical Fibers," IEEE Sensors Journal 12, 189-194 (2012).
[33] Chin, S., Primerov, N., and Thevenaz, L., "Photonic delay line for broadband optical signals, based on dynamic grating reflectors in fibers," 2010 36th European Conference and Exhibition on Optical Communication - (ECOC 2010), Torino, Italy, (2010).
[34] Santagiustina, M. and Ursini, L., "Dynamic Brillouin gratings permanently sustained by chaotic lasers", *Opt. Lett.* 37(5), 893-895 (2012)
[35] Antman, Y., Primerov, N., Sancho, J., Thevenaz, L., and Zadok, A., "Localized and stationary dynamic gratings via stimulated Brillouin scattering with phase modulated pumps," Optics Express 20, 7807-7821 (2012).
[36] Antman, Y., Primerov, N., Sancho, J., Thevenaz, L., and Zadok, A., "Variable delay using stationary and localized Brillouin dynamic gratings," Proceedings of Advances in Slow and Fast Light V, (SPIE Photonics West 2012, San-Francisco, CA)," Proc. SPIE 8273, 82730C1-82730C-8 (2012).
[37] Sancho, J., Primerov, N., Chin, S., Antman, Y., Zadok, A., Sales, S., and Thévenaz, L., "Tunable and reconfigurable multi-tap microwave photonic filter based on dynamic Brillouin gratings in fibers," Opt. Express 20, 6157-6162 (2012).
[38] Antman, Y., Primerov, N., Sancho, J., Thevenaz, L. and Zadok, A., "Long Variable Delay and Distributed Sensing Using Stationary and Localized Brillouin Dynamic Gratings", *Optical Fiber Communication Conference (OFC)*, JW2A.24 (2012)